

A Preliminary Step to Decipher an Enigma Using Time-of-Flight Sensor

Rohit Uppal*

Department of Electrical and Computer Engineering, University of Louisville



*Correspondence: r0uppa01@louisville.edu

Abstract: Refractive index (RI) was characterized from the slope of the linear fit of the measured perimeter of the loop of a waveguide vs. computed perimeter of the loop of the waveguide by using time-of-flight (TOF) sensor. The RI of uncladded commercially available waveguide was found to be 1.247 and 1.319 at 940 nm using ToF sensor and ellipsometer, respectively. The novel, simple and cost-effective technique may hold potential to initiate new avenues of research.

Classification: Waveguides, Elastomer, Time-of-Flight sensor

Keywords: Refractive Index, Waveguide, Time-of-Flight

Introduction

A change in refractive index (RI) reflects structural heterogeneity. RI is determined from relative permittivity (ϵ_r), the absorption coefficient (α) and wavelength (λ), as given in equation 1.

$$n^2 = \epsilon_r + (\lambda\alpha/4\pi)^2 \quad (1)$$

For measuring RI, thickness of the films has to be less than a few micrometers and need plane-parallel boundaries while using ellipsometer.(1) For characterizing RI using a confocal optical microscopy, both the phase and group refractive indices would have to be known.(2–5) The measurement depends upon the resolution in a heterodyne interference confocal microscopy.(6, 7) Specimen thickness has to be greater than the distance between the foci in case of bifocal optical coherence tomography.(8) For a transparent media, RI was determined using a laser meter.(9)

Time-of-flight (TOF) LiDAR has a laser emitter and single photon avalanche diode (SPAD). SPAD is an avalanche photon diode, which is biased higher than the breakdown voltage. As

single photon may trigger an avalanche, hence, SPAD can detect single photon.(10) The distance can be computed by measuring the time accurately between emission and detection of a precisely-controlled pulse.(11)

A novel and simple technique to characterize RI is proposed from the slope of the linear fit of the measured perimeter of the loop of a waveguide vs. computed perimeter of the loop of uncladded commercially available waveguide by using time-of-flight sensor.

Results and Discussion

Wave-Guide Parameter

The RI of the film of waveguides was found to be 1.319 ± 0.055 at 940 nm. The waveguide is highly amorphous, have low polarizability and hence, have low RI. As $V = 10079$, so multimode waveguide is capable of propagating a high data rate.

Loop Perimeter and Computation of Refractive Index

A part of the light is reflected at the interface of the laser emitter and the waveguide, and a part is transmitted. Intensity transmitted through the waveguide is calculated by equation 2.

$$I = I_0 e^{-\alpha c t / n L_m} \quad (2)$$

where α is the attenuation coefficient, L_m is the measured perimeter of the loop of a waveguide, and c is the speed of light.

It was assumed that in the absence of absorption the intensity of light does not change. Due to

the difference in the refractive indices of the waveguide and air, the transmitted fraction is reflected back.

Based on the premise that the slope of the linear fit of measured perimeter of the loop of a waveguide vs. computed perimeter of the loop of a waveguide represents a ratio of the flight times in air and in the waveguide, a very simple and novel technique to characterize RI is proposed, as given in an empirical equation 3.

$$n_w = c\tau n_a / L_m \quad (3)$$

Where, τ is the time taken by a pulse, which is reflected at the interface at the critical angle, to transmit through the waveguide, and n_w and n_a are the refractive indices of the waveguide and air.

For air, $L_m = c\tau$. For MatterHackers waveguide, average value of $c\tau/L_m$ of the linear fit of the measured perimeter of the loop of the waveguide vs. computed perimeter of the loop of the waveguide is 1.008 (Figure 1 and Table 1). The RI of air is 1.000272.(12)

Hence, the RI of the waveguide (n_w) is 1.247. Whereas RI using Woollam ellipsometer was found to be 1.319 ± 0.055 . The difference in the RI of the waveguide from the proposed method and Woollam ellipsometer could be attributed to that the light pulses within the waveguide propagate in different modes with different group velocities and so, have different flight times.

(13) Additionally, it was presumed that the intensity of light does not change in the absence of

absorption.

Material and Methods

Commercial Waveguide

MH Build Series is a clear thermoplastic elastomeric waveguide. It was purchased from MatterHackers, CA. The diameter and the density of the waveguide are 1.75 mm and 1.12 g/cc, respectively.

Wave-Guide Parameter (V)

A film of the waveguides was fabricated in an oven at 230 °C as discussed elsewhere.(14) The RI of the film was measured by using Woollam ellipsometer (Model HS-190). Propagation modes are characterized by wave-guide parameter (V).(14)

Loop Perimeter Computation

A loop of the uncladded waveguide was connected to time-of-flight sensor (VL53L0X) [Figure 2] at a bias voltage of 3.3V.(14) It is manufactured by STMicroelectronics, Geneva. It has a vertical cavity surface-emitting laser emitter, which emits a laser with a wavelength of 940 nm, and a SPAD. The photodetector is able to detect single photons with a temporal resolution of a few tens of picoseconds. The waveguides were cut by ten centimeters in steps and the loop perimeter was measured. The loop perimeter was computed by the time-of-flight sensor with an 8-bit microcontroller (Arduino Uno).

Acknowledgement

I gratefully acknowledge Dr. C.K. Harnett's help for allowing me to use a software. I thank Dr. Martin for measuring the RI and Paul Bupe for drawing a part of the schematic illustration for the computation of the perimeter.

Author Contributions: Conceptualization, Design of the Experiment, Investigation, Methodology, Conceiving Novel Method, Data Analysis, Writing-Original Draft, Review & Editing

Competing Interest Statement: The authors declare that they have no known competing financial interests or personal relationships that could have appeared to influence the work reported in this paper.

References

1. J.C. Charmet, P.G. de Gennes, Ellipsometric formulas for an inhomogeneous layer with arbitrary refractive-index profile. *J Opt Soc Am* **73**, 1777 (1983).
2. M.-T. Tsai, *et al.*, Defect detection and property evaluation of indium tin oxide conducting glass using optical coherence tomography. *Opt. Express* **19**, 7559–7566 (2011).
3. M. Haruna, *et al.*, Simultaneous measurement of the phase and group indices and the thickness of transparent plates by low-coherence interferometry. *Opt. Lett.* **23**, 966–968 (1998).
4. M. Ohmi, H. Nishi, Y. Konishi, Y. Yamada, M. Haruna, High-speed simultaneous measurement of refractive index and thickness of transparent plates by low-coherence interferometry and confocal optics. *Meas. Sci. Technol.* **15**, 1531–1535 (2004).
5. Y. Youk, *et al.*, “Refractive index and geometrical structure measurement of a core-doped photonic crystal fiber.” in *Photonic Crystal Materials and Devices IV*, SPIE Proceedings., A. Adibi, S.-Y. Lin, A. Scherer, Eds. (SPIE, 2006), p. 61281P.
6. T. Fukano, I. Yamaguchi, Separation of measurement of the refractive index and the geometrical thickness by use of a wavelength-scanning interferometer with a confocal microscope. *Appl. Opt.* **38**, 4065–4073 (1999).
7. Y. Watanabe, I. Yamaguchi, Digital Hilbert transformation for separation measurement of thicknesses and refractive indices of layered objects by use of a wavelength-scanning heterodyne interference confocal microscope. *Appl. Opt.* **41**, 4497–4502 (2002).
8. S.A. Alexandrov, A.V. Zvyagin, K.K.M.B.D. Silva, D.D. Sampson, Bifocal optical coherent refractometry of turbid media. *Opt. Lett.* **28**, 117–119 (2003).
9. K. Aoki, T. Mitsui, A tabletop experiment for the direct measurement of the speed of light. *Am J Phys* **76**, 812–815 (2008).
10. G. Chen, C. Wiede, R. Kokozinski, Data Processing Approaches on SPAD-Based d-TOF LiDAR Systems: A Review. *IEEE Sens. J.* **21**, 5656–5667 (2021).
11. S. Bellisai, *et al.*, Single-photon pulsed-light indirect time-of-flight 3D ranging. *Opt. Express* **21**, 5086–5098 (2013).
12. J.S. Jr, J.H. Zimmerman, Index of refraction of air. (2001).
13. L. Ibbotson, *The Fundamentals of Signal Transmission: Optical Fibre, Waveguides and Free Space.* (1998).
14. R. Uppal, K. Ajjarapu, K. Kate, C.K. Harnett, Low attenuation soft and stretchable elastomeric optical waveguides. *Mater Lett* **299**, 130079 (2021).

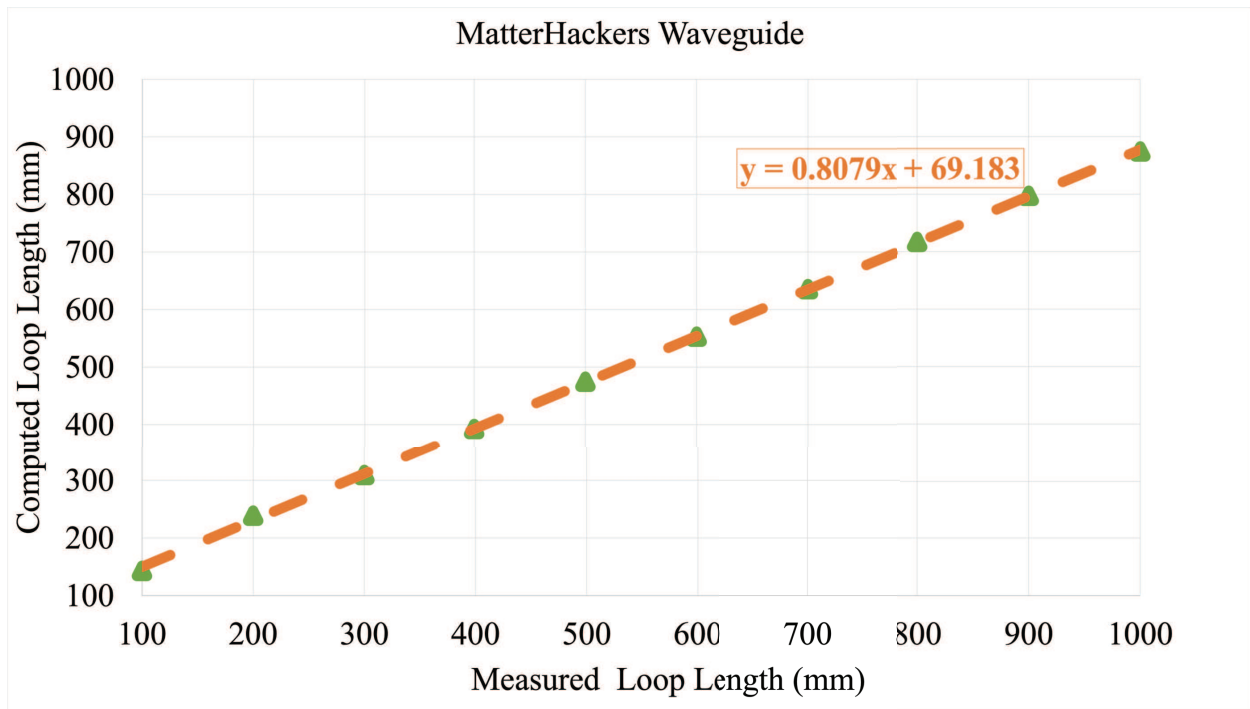


Figure 1: Computed distance at different loop perimeters of MatterHackers waveguide.

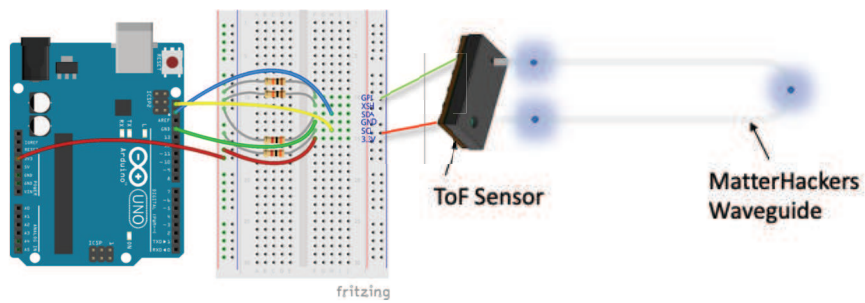


Figure 2: Schematic illustration for computation of the perimeter of the loop of a waveguide

Table 1: Measured and Computed Loop Perimeter of the Waveguide

| Measured Loop Perimeter (L_m) (mm) | Computed Loop Perimeter (L_c) (mm) | L_c/L_m |
|----------------------------------------|----------------------------------------|-----------|
| 1000 | 874.37 | 0.874 |
| 900 | 797.00 | 0.886 |
| 800 | 717.03 | 0.896 |
| 700 | 635.42 | 0.908 |
| 600 | 552.76 | 0.921 |
| 500 | 474.69 | 0.949 |
| 400 | 392.53 | 0.981 |
| 300 | 309.69 | 1.032 |
| 200 | 238.56 | 1.193 |
| 100 | 143.43 | 1.434 |